PHYSICAL REVIEW B **75**, 100401(R) (2007)

Commensurate fluctuations in the pseudogap and incommensurate spin-Peierls phases of TiOCl

J. P. Clancy,[1] B. D. Gaulin,[1,2] K. C. Rule,[1] J. P. Castellan,[1] and F. C. Chou[3]
[1]*Department of Physics and Astronomy, McMaster University, Hamilton, Ontario, Canada, L8S 4M1*
[2]*Canadian Institute for Advanced Research, 180 Dundas Street West, Toronto, Ontario, Canada, M5G 1Z8*
[3]*Center for Condensed Matter Sciences, National Taiwan University, Taipei 106, Taiwan*
(Received 16 January 2007; published 16 March 2007)

X-ray scattering measurements on single crystals of TiOCl reveal the presence of commensurate dimerization peaks within both the incommensurate spin-Peierls phase and the so-called pseudogap phase above T_{C2}. This scattering is relatively narrow in **Q**-space indicating long correlation lengths exceeding ~100 Å below $T^* \sim 130$ K. It is also slightly shifted in **Q** relative to that of the commensurate long range ordered state at the lowest temperatures, and it coexists with the incommensurate Bragg peaks below T_{C2}. The integrated scattering over both commensurate and incommensurate positions evolves continuously with decreasing temperature for all temperatures below $T^* \sim 130$ K.

DOI: 10.1103/PhysRevB.75.100401 PACS number(s): 75.25.+z, 75.40.Gb, 75.50.Xx

Low-dimensional quantum magnets with singlet ground states are of intense current interest due to the novelty of their ground states and their relationship to high temperature superconductivity.[1] Among quasi-one-dimensional antiferromagnets, much attention has focused on a small number of quasi-one-dimensional Heisenberg $S=1/2$ chain materials which undergo a spin-Peierls phase transition to a dimerized singlet ground state.[2] $CuGeO_3$ was the first inorganic material to display a spin-Peierls phase transition of $T_C \sim 14$ K.[3] Its discovery allowed studies of this exotic state in large single crystal form and also in the presence of dopants.[4] These works substantially informed the discussion on the nature of this quantum ground state. Earlier studies on organic spin-Peierls materials, such as TTF-CuBDT (Ref. 2) and MEM-$(TCNQ)_2$ (Ref. 5) also attracted great interest, but were more limited due to the low density of magnetic moments that these materials possess.

Recently, quantum magnets based on Ti^{3+} $(3d^1)$ have been shown to display unconventional spin-Peierls states. At low temperatures TiOCl and TiOBr both display dimerized magnetic singlet ground states. On increasing temperature both materials undergo discontinuous phase transitions at T_{C1} to incommensurate states closely related to the dimerized ground state.[6–11] On further raising the temperature, the incommensurate ordered phase undergoes an apparently continuous phase transition at T_{C2} to a disordered pseudogap phase. TiOCl displays a NMR signature within this pseudogap phase between T_{C2} and $T^* \sim 130$ K, similar to that observed in underdoped high temperature superconductors.[7] T_{C1} and T_{C2} occur at ~63 and 93 K, respectively, in TiOCl,[6,7,9,12,13] and at ~27 and 47 K in TiOBr.[10,11]

The spin-Peierls states in TiOCl and TiOBr possess significant and interesting differences from previously studied spin-Peierls materials. Their phase transition temperatures are higher by factors of between 2 and 4. Furthermore, the singlet-triplet gap deduced from NMR[7] and μSR measurements[14] on TiOCl below T_{C1} are ~430 and ~440 K, respectively. These are high compared with other spin-Peierls systems and with its own $T_{C1,C2}$; $\frac{2E_g}{k_B T_{C1,C2}} \sim 10-15$, as opposed to the conventional BCS value of 3.5 expected within mean field theory.[2]

TiOCl crystallizes into the orthorhombic FeOCl structure and is comprised of Ti-O bilayers separated by chlorine ions along the c-direction.[6,15] It displays room temperature lattice parameters of $a=3.79$ Å, $b=3.38$ Å, and $c=8.03$ Å.[15] At temperatures of 200 K and above its magnetic susceptibility, $\chi(T)$, can be described by an $S=1/2$ Heisenberg chain model, with a near-neighbor exchange constant $J=660$ K.[6] The implied reduction of the magnetic dimensionality of the Ti-O bilayers, from two to one, has been proposed as originating from ordering of Ti^{3+} orbital degrees of freedom.[6]

In this Rapid Communication we report x-ray scattering measurements on TiOCl which show commensurate fluctuations of a dimerized structure that first appear at $T^* \sim 130$ K, the onset of the pseudogap phase. We further show that the intensity and width of the scattering from these fluctuations peak at T_{C2}, but the commensurate fluctuations coexist with the incommensurate ordered structure for all temperatures above T_{C1}. Finally we show that the growth of the Q-integrated dimerization scattering is continuous at all temperatures measured.

Single crystal samples of TiOCl were grown by the chemical vapor transport method, as reported earlier.[6] The crystal studied had approximate dimensions of $2.0 \times 2.0 \times 0.1$ mm^3. The sample was mounted on the cold finger of a closed cycle refrigerator and aligned within a Huber four circle goniometer. Cu $K\alpha$ ($\lambda=1.54$ A) radiation from a rotating anode source was employed in all measurements reported. These measurements had a penetration depth of ~25 μm in TiOCl. The temperature of the sample was stabilized to $\sim \pm 0.01$ K.

X-ray scattering scans of the form $(H, 1.5, 1)$, $(2, K, 1)$, and $(2, 1.5, L)$ were performed around the commensurate dimerization wave vector (2, 1.5, 1) and several other equivalent ordering wave vectors at low temperatures. We ultimately focused around the (2, 1.5, 1) dimerization wave vector, as the intensity of the superlattice Bragg peaks was strongest there. Figures 1 and 2 show the H and K scans which were carried out as a function of temperature. Figure 1 shows a color contour map containing all of the H scans performed between 55 and 150 K, and the main qualitative features of this Rapid Communication can be found in it.

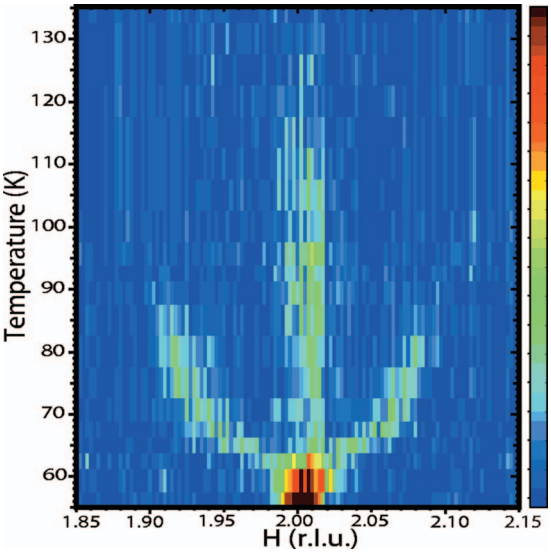

FIG. 1. (Color) A color contour map of x-ray scattering intensity as a function of temperature in TiOCl. H scans of the form (H, 1.5, 1) are shown with background scans at 200 K subtracted. One clearly observes commensurate dimerization scattering at (2, 1.5, 1) in both the incommensurate ($T_{C1} \sim 63$ K to $T_{C2} \sim 93$ K) and pseudogap phases (T_{C2} to $T^* \sim 130$ K).

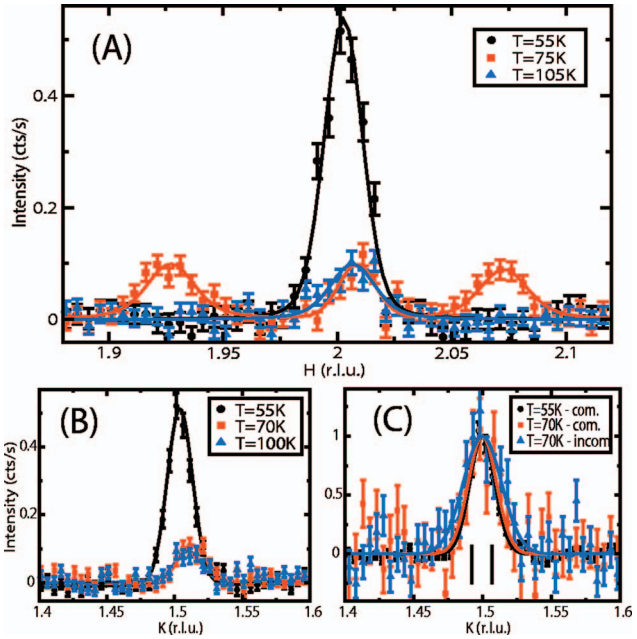

FIG. 2. (Color) (a) Representative H scans of the form (H, 1.5, 1). (b) Representative K scans of the form (2, K, 1). (c) K scans shown in (b) are scaled so that peak intensities are the same and are centered such that peaks occur at $K=1.5$. The incommensurate scattering at $T=70$ K is broader in K than either the commensurate scattering above or below T_{C1}. This is attributed to weak incommensuration along K, such that the incommensurate scattering occurs at ($2\pm\delta$, $1.5\pm\epsilon$, 1). The vertical lines indicate the expected position of the incommensurate peaks in K for $T=70$ K.

Figure 2 shows representative H and K scans at three temperatures—in the commensurate spin-Peierls phase at 55 K, the incommensurate phase at 75 K/70 K, and the pseudogap phase at 105 K.

All data sets have had a background data set, collected at 200 K, subtracted from them. This is necessary as weak $\lambda/2$ contamination of the incident x-ray beam produces Bragg scattering at the commensurate, (2, 1.5, 1) position in reciprocal space. This $\lambda/2$ scattering, whose strength is comparable to the λ scattering in the pseudogap phase ($\sim$0.1 counts/s), is temperature independent and can easily be subtracted off to reveal a background-free signal.

Several features are immediately clear from examination of Fig. 1. The previously observed incommensurate Bragg peaks[9] which appear continuously below $T_{C2} \sim 93$ K evolve towards the commensurate dimerization wave vector with decreasing temperature, giving rise to the transition to the commensurate, dimerized spin-Peierls state below $T_{C1} \sim 63$ K. However, most importantly, we observe commensurate scattering centered very near (2, 1.5, 1), which coexists with the incommensurate spin-Peierls state, and can be observed to temperatures as high as $T^* \sim 130$ K.

This commensurate dimerization scattering above T_{C1} has not been observed previously in either TiOCl or TiOBr, and it possesses several very interesting characteristics. Close examination of the detailed H and K scans shown in Fig. 2 reveals that this commensurate scattering is peaked close to, but not precisely at, the commensurate wave vector characterizing the low temperature dimerized state below T_{C1}. Figures 2(a) and 2(b) show this scattering peaks up at $\sim$ (2.005, 1.505, 1) rather than at (2, 1.5, 1). The incommensurate scattering we observe between T_{C1} and T_{C2} is also peaked up at ($2\pm\delta$, 1.5, 1); that is it is centered on $K=1.5$, like the low temperature commensurate scattering. Figure 2(c) shows scaled and centered K scans of the commensurate scattering in the low temperature phase at 55 K, as well as commensurate and incommensurate scattering between T_{C1} and T_{C2} at 70 K. We see that the incommensurate scattering at 70 K is broader in K than either the low temperature commensurate scattering or the commensurate scattering above T_{C1}. This is explained and indeed expected as a consequence of the known,[9] weak incommensuration along K, such that the precise incommensurate wave vector is ($2\pm\delta$, $1.5\pm\epsilon$, 1) with $\delta \sim 0.06$ and $\epsilon \sim 0.006$ for TiOCl at 70 K as shown in Figs. 2(b) and 2(c).[9] The incommensurate phase in TiOBr is characterized by a similar form of the incommensurate wave vector—with incommensuration in both H and K.[11] Our measurements see this as a broadening in wave vector K, rather than as distinct incommensurate peaks, due to the relatively low resolution of our measurements which integrate over this very weak ϵ-incommensuration.

The new commensurate scattering above T_{C1} in TiOCl is relatively sharp in **Q**-space at all temperatures measured, indicating correlation lengths in excess of $\sim$100 Å even within the pseudogap phase. This commensurate scattering is therefore distinct from conventional critical scattering [as measured around the *incommensurate* Bragg positions at and above T_{C2} in TiOBr (Ref. 11)] wherein the correlation lengths diverge at the phase transition, typically as power laws. However, critical fluctuations are usually small at $(T-T_C)/T_C \sim 0.1$, which corresponds to 9 K above a phase transition with $T_C \sim 90$ K. Figure 3 shows Γ, the wave-

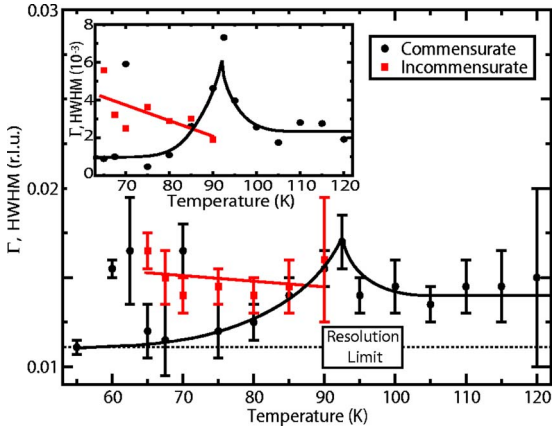

FIG. 3. (Color online) Γ, the H-width of the commensurate scattering above T_{C1}, as well as the incommensurate scattering between T_{C1} and T_{C2} is shown. The main panel shows widths extracted from Lorentzian fits to the raw data, while the inset shows intrinsic Lorentzian widths extracted from one-dimensional resolution-convoluted fits to the data. All lines provided are guides-to-the-eye.

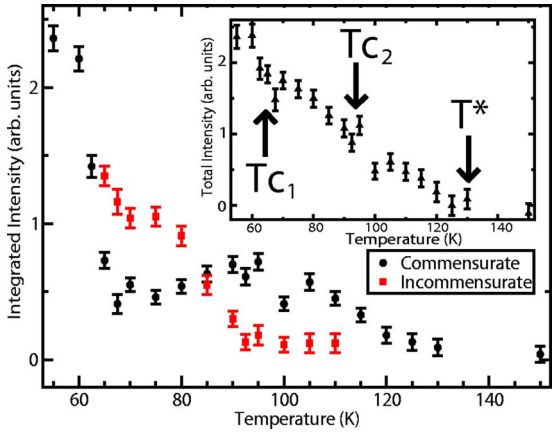

FIG. 4. (Color online) The integrated x-ray scattering around the commensurate position (2, 1.5, 1) is shown as a function of temperature with the black circles. The red squares show the integrated incommensurate scattering around ($H\pm\delta$, 1.5, 1). The inset shows the integrated scattering over all H in scans of the form (H, 1.5, 1) as a function of temperature. The growth of the Q-integrated scattering is continuous for all temperatures below $T^*\sim 130$ K.

vector H width of the new commensurate scattering, as well as of the incommensurate scattering, as a function of temperature. These widths were extracted from fits of the H scans, shown in Figs. 1 and 2, to a Lorentzian form for the scattering. The main panel shows fits to the raw data itself, while the inset shows the intrinsic width of the Lorentzian describing the scattering, convoluted in one dimension by the experimental resolution function appropriate to the measurement. This result shows that the new commensurate scattering above T_{C1} has a narrow but nonresolution limited line shape for all temperatures above T_{C1}. The width of the scattering, and hence the inverse correlation length, peak near T_{C2}. The same trend is seen when a resolution convolution of the scattering is explicitly included to extract quantitative estimates of the correlation lengths. We see that typical correlation lengths away from T_{C2} are $\xi_a\sim 1$/half width at half maximum $\sim 1/\left(\frac{2\pi}{a}\times 0.002\right)\sim 300$ Å, dropping to ~ 100 Å in the vicinity of T_{C2}.

We therefore conclude that the new commensurate scattering above T_{C1} is due to fluctuations, rather than long range order (LRO). This is consistent with NMR measurements[7] which show static LRO to occur only below T_{C2}. In addition, while several experimental techniques show evidence for the pseudogap phase below T^*, bulk characterization by susceptibility[6,12] and heat capacity[12,13] provide no evidence of an additional phase transition above T_{C2}. Figure 3 also shows the analysis for Γ, the H-width of the incommensurate scattering between T_{C1} and T_{C2}. This indicates that the scattering is broader than resolution-limited, on the basis of comparison with the commensurate LRO scattering at $T=55$ K. The interpretation of the width of the incommensurate scattering is complicated by the weak ϵ-incommensuration along K, which may induce a finite H-width to the measured scattering by virtue of our resolution. However, the most straightforward interpretation of these results is that the incommensurate scattering also displays a long but noninfinite correlation length ~ 200 Å because coexisting commensurate fluctuations and incommensurate order compete against each other between T_{C1} and T_{C2}. Examination of their temperature dependencies also supports such an interpretation.

The temperature dependence of the commensurate and incommensurate dimerization scattering is shown in Fig. 4. This integrated intensity is obtained by performing integrations over a small range of wave vectors around either the incommensurate or commensurate wave vectors such that all of the relevant scattering is captured. One clearly sees the continuous rise of the incommensurate intensity near $T_{C2}\sim 93$ K, and the discontinuous rise in the commensurate scattering near $T_{C1}\sim 63$ K. Most importantly, one sees the continuous rise of the commensurate fluctuation scattering near $T^*\sim 130$ K, which peaks at T_{C2} and decreases slowly until T_{C1}.

We conclude that the pseudogap phase between T^* and T_{C2} is characterized by the growth of commensurate dimerization fluctuations with correlation lengths of many unit cells. Below T_{C2} incommensurate Bragg-like scattering coexists with the commensurate fluctuations. The concomitant rise of the incommensurate scattering intensity along with the peak in the temperature dependence of the integrated intensity of the commensurate fluctuations at T_{C2} suggests a competition between these two states in the regime between T_{C1} and T_{C2}.

Related phenomena may occur in Mg-doped $CuGeO_3$,[16] wherein a spin gap is established at a higher temperature than that which characterizes the spin-Peierls LRO. This pseudogap regime displays commensurate dimerization scattering, with long, but not infinite, correlation lengths, and it has been attributed to impurity-induced interchain interactions.

It is also straightforward to integrate up all the scattering in scans of the form shown in Figs. 1 and 2, covering both the commensurate and incommensurate wave vectors. This temperature dependence is shown in the inset to Fig. 4. Remarkably this integrated intensity varies smoothly with temperature from T^*, with no sign of a discontinuity at T_{C1}. The temperature dependence of the intensity of the commensu-

rate LRO scattering below T_{C1} is known to be almost temperature independent.[9] Hence we see a linear growth in the overall dimerization scattering below T^*, saturating into a commensurate LRO spin-Peierls state below T_{C1}.

Most phase transitions are characterized by an order parameter and order parameter fluctuations, both of which possess the same wave vector. However, there are examples of materials whose fluctuations above a phase transition occur at a different wave vector than that which characterizes the LRO state below T_C. UNi_2Al_3, for example, exhibits an incommensurate magnetically ordered state below $T_N \sim 4.6$ K (Ref. 17) which is preceded by dynamic short range fluctuations at the commensurate magnetic wave vector[18] which characterizes the ordered state in its sister compound UPd_2Al_3.[19] This is believed to arise due to competition between Ruderman-Kittel-Kasuya-Yosida interactions and Kondo screening in this heavy fermion metal. Competing finteractions leading to frustration are widely discussed in the context of the incommensurate spin-Peierls phases of both TiOCl and TiOBr. Ruckamp *et al.*,[12] for example, have proposed that the incommensurate order in TiOCl originates from competing in-phase and out-of-phase arrangements of dimers within the Ti-O layers which make up the bilayers. Our data suggests that such competing interactions not only give rise to the incommensurate spin-Peierls state, but also lead to contending yet coexisting ground states between T_{C1} and T_{C2}.

To conclude, we have observed commensurate dimerization scattering which first appears at the onset of the pseudogap phase, $T^* \sim 130$ K, and which coexists with the incommensurate state below T_{C2}. This commensurate scattering exhibits long, but finite correlation lengths at all temperatures measured, and both its integrated intensity and inverse correlation length peak at T_{C2}. Although similar commensurate scattering has yet to be observed in TiOBr, the combination of competing interactions and incommensurate structure which is common to both materials could easily give rise to an analogous effect.

We wish to acknowledge very helpful discussions with T. Imai. This work was supported by NSERC of Canada and NSC of Taiwan.

[1] See, for example, E. Dagotto and T. M. Rice, Science **271**, 618 (1996); *Dynamical Properties of Unconventional Magnetic Systems*, edited by A. T. Skjeltorp and D. Sherrington, NATO ASI Series, Series E, Applied Sciences Vol. 349 (Kluwer Academic Publishers, Boston, 1998).

[2] J. W. Bray, L. V. Interrante, I. S. Jacobs, and J. C. Bonner, in *Extended Linear Chain Compounds*, edited by J. S. Miller (Plenum Press, New York, 1983), Vol. 3, p. 353, and references therein.

[3] M. Hase, I. Terasaki, and K. Uchinokura, Phys. Rev. Lett. **70**, 3651 (1993); J. P. Pouget, L. P. Regnault, M. Ain, B. Hennion, J. P. Renard, P. Veillet, G. Dhalenne, and A. Revcolevschi, *ibid.* **72**, 4037 (1994).

[4] M. Hase, I. Terasaki, Y. Sasago, K. Uchinokura, and H. Obara, Phys. Rev. Lett. **71**, 4059 (1993); S. B. Oseroff, S. W. Cheong, B. Aktas, M. F. Hundley, Z. Fisk, and L. W. Rupp, Jr., *ibid.* **74**, 1450 (1995); M. D. Lumsden, B. D. Gaulin, and H. Dabkowska, Phys. Rev. B **58**, 12252 (1998).

[5] B. van Bodegom, B. C. Larson, and H. A. Mook, Phys. Rev. B **24**, 1520 (1981); M. D. Lumsden and B. D. Gaulin, *ibid.* **59**, 9372 (1999), and references contained therein.

[6] A. Seidel, C. A. Marianetti, F. C. Chou, G. Ceder, and P. A. Lee, Phys. Rev. B **67**, 020405(R) (2003).

[7] T. Imai and F. C. Chou, cond-mat/0301425 (unpublished).

[8] M. Shaz, S. van Smaalen, L. Palatinus, M. Hoinkis, M. Klemm, S. Horn, and R. Claessen, Phys. Rev. B **71**, 100405(R) (2005).

[9] A. Krimmel, J. Strempfer, B. Bohnenbuck, B. Keimer, M. Hoinkis, M. Klemm, S. Horn, A. Loidl, M. Sing, R. Claessen, and M. v. Zimmermann, Phys. Rev. B **73**, 172413 (2006).

[10] P. Lemmens, K. Y. Choi, R. Valenti, T. Saha-Dasgupta, E. Abel, Y. S. Lee, and F. C. Chou, New J. Phys. **7**, 74 (2005).

[11] T. Sasaki, M. Mizumaki, T. Nagai, T. Asaka, K. Kato, M. Takata, Y. Matsui, and J. Akimitsu, J. Phys. Soc. Jpn. **74**, 2185 (2005).

[12] R. Ruckamp, J. Baier, M. Kriener, M. W. Haverkort, T. Lorenz, G. S. Uhrig, L. Jongen, A. Moller, G. Meyer, and M. Gruninger, Phys. Rev. Lett. **95**, 097203 (2005).

[13] J. Hemberger, M. Hoinkis, M. Klemm, M. Sing, R. Claessen, S. Horn, and A. Loidl, Phys. Rev. B **72**, 012420 (2005).

[14] P. J. Baker, S. J. Blundell, F. L. Pratt, T. Lancaster, M. L. Brooks, W. Hayes, M. Isobe, Y. Ueda, M. Hoinkis, M. Sing, M. Klemm, S. Horn, and R. Claessen, Phys. Rev. B **75**, 094404 (2007).

[15] H. Schafer, F. Wartenpfuhl, and E. Weise, Z. Anorg. Allg. Chem. **295**, 268 (1958).

[16] Y. J. Wang, V. Kiryukhin, R. J. Birgeneau, T. Masuda, I. Tsukada, and K. Uchinokura, Phys. Rev. Lett. **83**, 1676 (1999).

[17] A. Schroder, J. G. Lussier, B. D. Gaulin, J. D. Garrett, W. J. L. Buyers, L. Rebelsky, and S. M. Shapiro, Phys. Rev. Lett. **72**, 136 (1994).

[18] B. D. Gaulin, M. Mao, C. R. Wiebe, Y. Qiu, S. M. Shapiro, C. Broholm, S.-H. Lee, and J. D. Garrett, Phys. Rev. B **66**, 174520 (2002).

[19] A. Krimmel, P. Fischer, B. Roessli, H. Maletta, C. Geibel, C. Schank, A. Grauel, A. Loidl, and F. Stegich, Z. Phys. B: Condens. Matter **86**, 161 (1992).